Cavity Ring-Down Spectroscopy of the Benzyl Radical

Kenichi Tonokura* and Mitsuo Koshi

Department of Chemical System Engineering, School of Engineering, The University of Tokyo, 7-3-1 Hongo, Bunkyo-ku, Tokyo 113-8656, Japan

Received: October 22, 2002; In Final Form: February 14, 2003

The electronic absorption spectrum of the benzyl radical ($C_6H_5CH_2^{\bullet}$) has been measured in the region of the vibrationally mixed $1^2A_2-2^2B_1$ excited states near 450 nm by cavity ring-down spectroscopy (CRDS) in 20 Torr of argon or nitrogen diluents at 298 K. The absorption cross section was determined from the CRDS absorption and the rates of radical−radical cross reactions. At 447.7 nm, $\sigma_{benzyl} = (2.2 \pm 0.8) \times 10^{-18}$ cm^2 molecule^{-1} (base e). The rate constant for the reaction of benzyl radicals with Cl atoms was derived during the modeling: $k(C_6H_5CH_2 + Cl) = (2.5 \pm 1.0) \times 10^{-10}$ cm^3 molecule^{-1} s^{-1}. Time-dependent density functional theory calculations support the interpretation of the absorption spectrum of the benzyl radical.

Introduction

Aromatic compounds such as benzene, toluene, and the xylenes are of great interest in the chemistry of the urban atmosphere because of their abundance in motor vehicle emissions and because of their reactivity with respect to ozone and organic aerosol formation. Of the aromatic compounds, toluene has the highest typical ambient concentration (∼100 ppb) in urban areas.[1] Toluene is degraded in the troposphere via reaction with OH radicals, and about 10% of the reaction proceeds via H-atom abstraction from the methyl group, leading to the formation of the benzyl radical ($C_6H_5CH_2^{\bullet}$). Benzaldehyde and benzyl nitrate are produced after benzyl formation by following reactions involving the benzyl peroxy radical. Spectroscopic and kinetic data concerning benzyl radicals are needed to understand the environmental impact of vehicle exhaust.

In a pioneering gas-phase flash photolysis study, Porter and Ward established that benzyl radicals have weak absorption bands in the visible region (430−455 nm).[2] There are two degenerate low-lying excited states of A_2 and B_1 symmetry near 450 nm.[3] Using a two-mode vibronic coupling model, Cossart-Magos and Leach[4] carried out a rotational contour analysis of the emission spectra at room temperature that clearly assigned these to an excitation from the zero vibrational level of the 2^2B_1 state to a vibrational level of the 1^2A_2 state. Cossart-Magos and Goetz[5] reported the rotational analysis of the visible absorption bands and a determination of the variations of the rotational constants accompanying the vibronic transitions corresponding to each band. Laser-induced fluorescence (LIF) and multiphoton ionization (MPI) methods have been applied to study the vibronic coupling mechanism in the $1^2A_2-2^2B_1$ excited states of the benzyl radical.[6−15] Eiden and Weisshaar[14] have compiled most of the available experimental and theoretical data and have modeled a scheme for the vibronic coupling mechanism in the 1^2A_2 and 2^2B_1states of the benzyl radical. The visible and UV absorption spectra of benzyl radicals in low-temperature rare-gas matrices have been the subject of several experimental investigations.[16−18]

The geometric and electronic structure of the ground and lower excited states of the benzyl radical has been the subject of theoretical studies. Rice et al.[19] performed multiconfiguration ab initio calculations on ground and lower excited states of the benzyl radical. Hiratsuka et al.[20] reported energy levels and oscillator strengths of the benzyl radicals by CNDO/S CI calculations. Negri et al.[21] studied the absorption and emission spectra including the effects of vibronic coupling by semiempirical theory. Gunion et al.[22] reported the geometry and harmonic frequencies for the benzyl radical at the HF/6-31G(d,p) level of theory.

Despite numerous studies, significant uncertainties remain in our understanding of the spectroscopy and kinetics. For example, the absolute strength of the visible absorption spectrum is unknown. In this study, we present the absolute absorption spectrum of the benzyl radical in the visible region measured by cavity ring-down spectroscopy (CRDS). The kinetics of reaction of benzyl radicals and Cl atoms was also investigated. Time-dependent density functional theory (TD-DFT) calculations were performed to support the spectroscopic work.

Experimental and Computational Details

CRDS has been well established in the field of chemical kinetic study.[23] The laser photolysis/CRDS apparatus that was used is described in detail elsewhere.[24] The system employs two pulsed lasers. The first laser (193.3-nm output of an excimer laser, Lambda Physik COMPex 110) was used to photolyze a suitable precursor to generate benzyl radicals. The photolysis laser was 3 cm wide, and the average photon flux across the entire sample was uniform within 10%. The photolysis laser was 3 cm wide. The second laser (Lambda Physik LPD 3002; coumarin 450, pumped by the 308-nm output of an excimer laser Lambda Physik LPX 110) was used to probe the absorption of the benzyl radical. The photolysis laser entered the flow cell at right angles to the cavity and overlapped the probe laser beam at the center of the flow cell. The probe laser beam was injected through one of two high-reflectivity mirrors that made up the ring-down cavity. The mirrors (Research Electro Optics) had a specified maximum reflectivity of 0.9995 at 457 nm, a diameter of 25.4 mm, and a radius of curvature of 1.2 m and were

* Corresponding author. E-mail: tonokura@reac.t.u-tokyo.ac.jp.

10.1021/jp027280k CCC: $25.00
Published on Web 05/06/2003

mounted 0.625 m apart. Light leaking from one of the mirrors of the ring-down cavity was detected by a photomultiplier tube (PMT; Hamamatsu R955). The decay of the light intensity was recorded using a digital oscilloscope (Tektronix TDS 520C) and transferred to a personal computer. The decay of the light intensity is given by the expression

$$I(t) = I_0 \exp\left(-\frac{t}{\tau}\right) = I_0 \exp\left(-\frac{t}{\tau_0} - \sigma nc\left(\frac{L_R}{L}\right)t\right)$$

where I_0 and $I(t)$ are the intensities of light at time 0 and t, respectively. τ_0 is the empty cavity ring-down time (4 μs at 447 nm), L_R is the length of the reaction region (3 cm), L is the cavity length (0.625 m), and τ is the measured cavity ring-down time. n and σ are the concentration and absorption cross sections, respectively, of the species of interest, and c is the velocity of light. Absorption spectra were obtained by scanning the wavelength of the probe laser with a spectral resolution of 0.1 cm^{-1}. For time-dependent studies, the delay time between the photolysis and probe laser beams was controlled by a pulse generator (Stanford Research Systems DG535). The initial benzyl concentrations were typically in the range of $(1-10) \times 10^{13}$ molecules cm^{-3} with precursor concentrations on the order of 10^{14} molecules cm^{-3} and a laser photon density of $\sim 5 \times 10^{15}$ photons cm^{-2}. The detection limit of the benzyl radical with the present apparatus is estimated to be $\sim 10^{11}$ molecules cm^{-3}.

The reaction cell was evacuated by a combination of an oil rotary pump with a liquid-nitrogen trap. The pressure in the cell was monitored by an absolute pressure gauge (MKS Baratron 622A). Gas flows were measured and regulated by mass flow controllers (Kofloc 3650). A slow flow of nitrogen or argon diluent gases was introduced at both ends of the ring-down cavity close to the mirrors and photolysis-beam entrance windows to minimize deterioration caused by exposure to reactants and products. Ethylbenzene (Aldrich, 99.8%) and benzyl chloride (Aldrich, 99%) were used as the photolytic precursor for benzyl radicals and were introduced into the reaction cell by passing a diluent gas. The total flow rate was kept constant at 1000 sccm. Reagent concentrations were calculated from the flow rates and total pressure. Spectroscopic and kinetic experiments were performed using a laser repetition of 1−5 Hz to ensure the removal of the reacted mixture and the replenishment of the gas sample between successive laser shots. Ethylbenzene and benzyl chloride were freeze−pump−thawed in liquid nitrogen to remove volatile contaminants.

The equilibrium geometry of the ground state of the benzyl radical was optimized by employing hybrid density functional theory B3LYP based on Becke's three-grid integration[25] and exchange functional and the correction functional of Lee, Yang, and Parr[26] with Dunning's correction-consistent aug-cc-pVDZ basis set.[27] Electronic transitions of the benzyl radical were investigated by employing TD-DFT calculations.[28,29] The calculations were based on the $^2B_1$ ground-state equilibrium.[3] C_{2v} molecular symmetry was assumed for the equilibrium geometry of the ground state. Calculations were carried out using the Gaussian 98[30] and Q-Chem program packages.[31]

Results and Discussion

The laser photolysis experiments were performed to produce benzyl radical and to characterize its absorption spectrum in the spectral range 445−455 nm. In these experiments benzyl radicals were generated from the 193 nm excimer laser photolysis of $C_6H_5CH_2X$.

$$C_6H_5CH_2X + 193.3\ nm \rightarrow C_6H_5CH_2 + X \qquad X = CH_3, Cl \qquad (R1)$$

The dominant channel of ethylbenzene following the 193-nm photoexcitation is the C−C bond cleavage,[32] and the dissociation rate is $2 \times 10^7\ s^{-1}$ at 0 Torr.[33,34] The H-atom elimination channel is negligibly small.[35] Hippler et al.[34,36,37] reported the pressure dependence of the quantum yield for benzyl formation $\phi(p)$ in the 193.3-nm photolysis of ethylbenzene. Under our experimental conditions ($p = 20$ Torr), ϕ is 0.6.[38] Ichimura et al.[39] reported that the quantum yield of photodissociation of benzyl formation in the photoexcitation of benzyl chloride to the S_3 state at 184.9 nm was 0.9. Because benzyl chloride is also excited to the S_3 state at 193.3-nm photoexcitation, the quantum yield for benzyl formation can be assumed to be 0.9. They also estimated the photodissociation rate to be $10^{10}\ s^{-1}$. The initial benzyl concentration in the photolysis experiments is estimated from the relation

$$[C_6H_5CH_2]_0 = N_p[C_6H_5CH_2X]\sigma^{193}_{C_6H_5CH_2X}\phi \qquad (1)$$

where $[C_6H_5CH_2X]$ and σ are the benzyl precursor concentration and absorption cross-section ($\sigma_{C_6H_5CH_2CH_3} = 1.9 \times 10^{-17}$ cm^2 $molecule^{-1}$,[37] $\sigma_{C_6H_5CH_2Cl} = 2.7 \times 10^{-17}$ cm^2 $molecule^{-1}$ [40]), respectively, and N_p is the number density of laser photons as determined from laser-pulse energy measurements.

Figure 1 shows the absorption spectrum of the benzyl radical produced in the 193.3-nm photolysis of ethylbenzene. The same absorption spectrum was observed following the 193.3-nm photolysis of benzyl chloride. The spectrum feature did not vary on the time scale of the measurements. Plots of absorbance versus photolysis laser power had a slope of 1.0 ± 0.1, indicating that the absorbing species is formed in a one-photon process. The peak positions in the spectrum agree with the electronic absorption spectrum ascribed to a visible electronic transition of the benzyl radical with a band origin at 22 002 cm^{-1} reported by Porter and Ward.[2] This absorption band has been assigned to the excitation of vibrationally mixed $1^2A_2-2^2B_1$ excited states. Table 1 shows the calculated and observed electronic transitions of the benzyl radical. Two close-lying electronic states (1^2A_2 and 2^2B_1) in the visible region and two intense transitions ($2^2A_2 \leftarrow 1^2B_1$ and $4^2B_2 \leftarrow 1^2B_1$) in the UV region are calculated at the TD-B3LYP/aug-cc-pVDZ level of theory. The TD-DFT energies agree remarkably well with experimental values.

TABLE 1: Benzyl Radical Excitation Energies, Oscillator Strengths, and Absorption Cross Sections

	calculated		observed	
state	energy (10^3 cm^{-1})	f [a]	energy (10^3 cm^{-1})	σ (10^{-18} cm^2 $molecule^{-1}$)
1^2A_2	25.4	0.0004	22.4	2.2 ± 0.8[b]
2^2B_1	27.2	0.0024		
2^2A_2	30.4	0.0258	32.8	35 ± 9,[c] 28 ± 6[d]
3^2B_1	34.0	0.0035		
4^2B_1	38.1	0.2950	39.5	110 ± 30,[c] 107 ± 21[d]

[a] Oscillator strength for the electronic transition. [b] This work. [c] Reference 50. [d] Reference 51.

Figure 2a and b shows the transient absorption at 447.7 nm observed as a function of time following the 193.3-nm photolysis of mixtures containing either $C_6H_5CH_2CH_3$ or $C_6H_5CH_2Cl$ in 20 Torr of nitrogen diluent at 298 K. The transient absorption

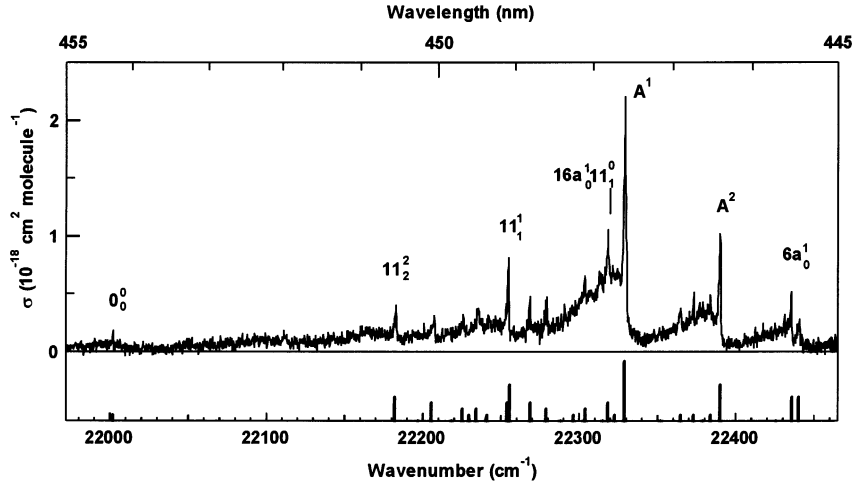

Figure 1. Absorption spectrum of the benzyl radical observed from the 193.3-nm photolysis of ethylbenzene. The time delay between the photolysis and probe laser beams was 10 μs. The lower stick spectrum shows the positions and relative intensities of the benzyl radical absorption peaks reported by Porter and Ward.[2]

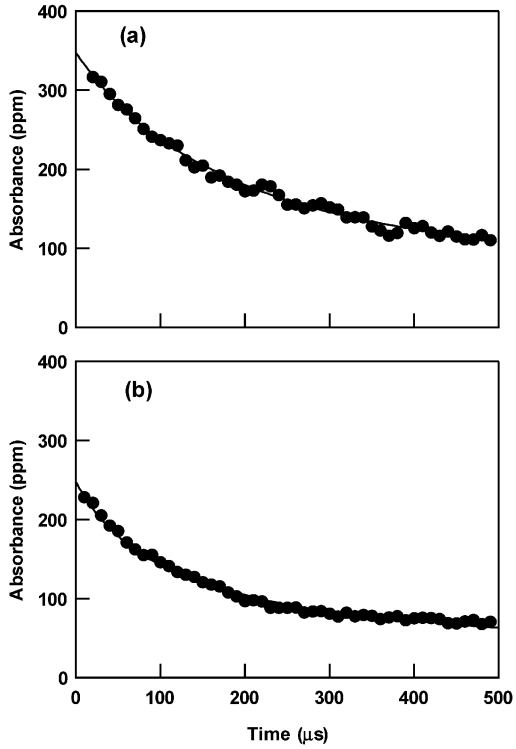

Figure 2. Absorbance at 447.7 nm by benzyl radicals following the 193.3-nm photolysis of (a) ethylbenzene and (b) benzyl chloride in 20 Torr of nitrogen diluent versus the time delay between photolysis and the probe laser. The solid curves are fits to the data. (See the text for details.)

profiles in Figure 2 can be used to extract information concerning the absorption cross section and reaction kinetics of benzyl radicals.[24] When the probe-laser bandwidth is narrower than the width of the absorption feature of interest, the absorption measurements in CRDS provide accurate measurements of the number densities.[41] Because the probe-laser bandwidth is less than one tenth of the width of the absorption feature at 447.7 nm, accurate measurements of benzyl radical concentration should be provided in the present experiments. As mentioned above, the benzyl radical quantum yields following the 193.3-nm photoexcitation of $C_6H_5CH_2CH_3$ and $C_6H_5CH_2Cl$ are 0.6 (20 Torr) and 0.9, respectively. Photolyzing $C_6H_5CH_2X$ (X = CH_3 or Cl) gives rise to equal concentrations of benzyl radicals and methyl radicals or chlorine atoms, which can then undergo self-reaction, cross reaction, and reaction with $C_6H_5CH_2X$.

$$C_6H_5CH_2 + C_6H_5CH_2 \rightarrow \text{products} \quad \text{(R2)}$$

$$C_6H_5CH_2 + X \rightarrow \text{products} \quad \text{(R3)}$$

$$X + X \rightarrow X_2 \quad \text{(R4)}$$

$$C_6H_5CH_2 + C_6H_5CH_2X \rightarrow \text{products} \quad \text{(R5)}$$

$$X + C_6H_5CH_2X \rightarrow \text{products} \quad \text{(R6)}$$

Tables 2 and 3 present the reaction mechanisms of the benzyl radicals following 193-nm photolysis of ethylbenzene and benzyl chloride. Recombination rate constants of the benzyl radicals have been measured over the range of 400−520 K and were found to be independent of temperature over the range; $k_2 = (2.9 \pm 0.3) \times 10^{-11}$ cm^3 molecule^{-1} s^{-1}.[42] We used this value in the kinetic model. Benzyl radicals react very slowly with aromatic compounds such as $C_6H_5CH_2CH_3$ and $C_6H_5CH_2Cl$;[34,43] reaction (R5) is not important in the present work.

The cross reaction of benzyl with methyl (reaction R3) proceeds with a rate constant of 1.4×10^{-11} cm^3 molecule^{-1} s^{-1}.[37] The recombination of methyl radicals via reaction R4 is well established: $k_{4,\text{methyl}}$ (20 Torr) = 5.2×10^{-11} cm^3 molecule^{-1} s^{-1}.[44] Methyl radicals react very slowly with aromatic compounds such as benzene and toluene (rate constants are less than 10^{-16} cm^3 molecule^{-1} s^{-1} at 298 K[45,46]); reaction R6 would be not significant in the ethylbenzene system.

In the benzyl chloride photolysis, the recombination of Cl atoms via reaction R4 in 20 Torr of diluent gases proceeds slowly (pseudo-second-order rate constants of approximately 10^{-14} cm^3 molecule^{-1} s^{-1} [47]); reaction R4 is not important on the time scale of the present experiments (<1 ms). The reaction of Cl atoms with $C_6H_5CH_2Cl$ via reaction R6 proceeds with a rate constant of $(9.6 \pm 0.6) \times 10^{-12}$ cm^3 molecule^{-1} s^{-1}.[48] There are two reported values of $k_3(C_6H_5CH_2 + Cl)$: 2.1×10^{-10} cm^3 molecule^{-1} s^{-1} [49] and $(6.9 \pm 1.4) \times 10^{-10}$ cm^3 molecule^{-1} s^{-1}.[50]

To derive the value for σ(447.7 nm), the observed benzyl radical decays such as those shown in Figure 2; the coupled

TABLE 2: Reactions Used in the Modeling of the Benzyl Radical Kinetics in the 193-nm Photolysis of Ethylbenzene

reaction	rate constant (cm^3 $molecule^{-1}$ s^{-1})	refs
$C_6H_5CH_2CH_3 + 193.3\ nm \rightarrow C_6H_5CH_2 + CH_3$	$(2.3 \pm 0.2) \times 10^7\ s^{-1}$, $\phi = 0.6$ (20 Torr)	34, 38
$C_6H_5CH_2 + C_6H_5CH_2 \rightarrow$ products	$(2.9 \pm 0.3) \times 10^{-11}$	42
$C_6H_5CH_2 + CH_3 \rightarrow$ products	1.4×10^{-11}	37
$CH_3 + CH_3 \rightarrow C_2H_6$	5.2×10^{-11} (20 Torr)	44

TABLE 3: Reactions Used in the Modeling of the Benzyl Radical Kinetics in the 193-nm Photolysis of Benzyl Chloride

reaction	rate constant (cm^3 $molecule^{-1}$ s^{-1})	refs
$C_6H_5CH_2Cl + 193.3\ nm \rightarrow C_6H_5CH_2 + Cl$	$10^{10}\ s^{-1}$, $\phi = 0.9$	39
$C_6H_5CH_2 + C_6H_5CH_2 \rightarrow$ products	$(2.9 \pm 0.3) \times 10^{-11}$	42
$C_6H_5CH_2 + Cl \rightarrow$ products	$(2.5 \pm 1.0) \times 10^{-10}$	this study
$C_6H_5CH_2Cl + Cl \rightarrow$ products	$(9.6 \pm 0.6) \times 10^{-12}$	48

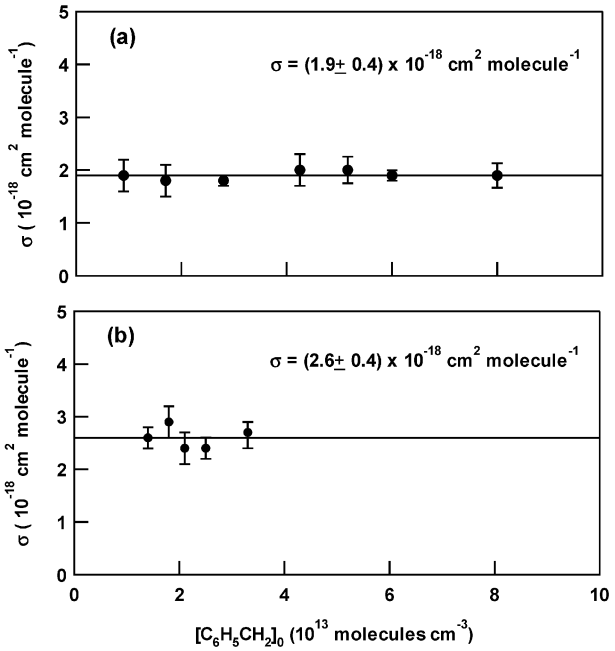

Figure 3. Plots of calculated absorption cross sections at 447.7 nm as a function of $[C_6H_5CH_2]_o$ in experiments using (a) $(3-10) \times 10^{14}$ molecule cm^{-3} of ethylbenzene and (b) $(1-3) \times 10^{14}$ molecule cm^{-3} of benzyl chloride with laser photolysis energies of ~5.0 mJ cm^{-2} $pulse^{-1}$.

differential equations describing the loss of $C_6H_5CH_2$ radicals and CH_3 radicals in the ethylbenzene system were solved by numerical integration routines.[24] Two parameters were varied simultaneously to provide the best fit: $[C_6H_5CH_2]_o = [CH_3]_o$ and σ(447.7 nm). The rate constant of $k_3(C_6H_5CH_2 + Cl)$ is added as a fitting parameter in the benzyl chloride system. The curves in Figure 2 are fits to the data that show that the model provides a good description of the experimental observations. Experiments employing $C_6H_5CH_2CH_3$ photolysis gave a value of $\sigma(447.7\ nm) = (1.9 \pm 0.4) \times 10^{-18}$ cm^2 $molecule^{-1}$. Experiments employing $C_6H_5CH_2Cl$ photolysis gave values of $k_3(C_6H_5CH_2 + Cl) = (2.5 \pm 1.0) \times 10^{-10}$ cm^3 $molecule^{-1}$ s^{-1} and $\sigma(447.7\ nm) = (2.6 \pm 0.4) \times 10^{-18}$ cm^2 $molecule^{-1}$. The values of σ(447.7 nm) derived from experiments employing $C_6H_5CH_2CH_3$ and $C_6H_5CH_2Cl$ photolysis were indistinguishable within the experimental uncertainties. The variation of the initial radical concentration by an order of magnitude had no discernible impact on the values of $k_3(C_6H_5CH_2 + Cl)$ or σ(447.7 nm) (see Figure 3) that were returned from the fitting procedure. As another approach, the absorption cross section can be estimated directly from the initial absorbance A_0, $[C_6H_5CH_2]_0$, and L_R:

$$A_0 = \sigma_{C_6H_5CH_2}[C_6H_5CH_2]_0 L_R \qquad (2)$$

$[C_6H_5CH_2]_0$ can be estimated from eq 1. Using this approach, we derived values of $\sigma(447.7\ nm) = (1.7 \pm 0.4) \times 10^{-18}$ cm^2 $molecule^{-1}$ for the ethylbenzene precursor and $(2.8 \pm 1.0) \times 10^{-18}$ cm^2 $molecule^{-1}$ for the benzyl chloride precursor. The values of σ (447.7 nm) obtained using the two different approaches are indistinguishable within the experimental uncertainties. We recommend quoting the mean value of the two approaches, σ (447.7 nm) $= (2.2 \pm 0.8) \times 10^{-18}$ cm^2 $molecule^{-1}$, as the best working value of the benzyl absorption cross section at 447.7 nm. Because this is the first determination of an absolute absorption cross section of the benzyl radical in the visible region in the gas-phase, comparable literature values are not obtained.

The A^1 and A^2 bands in the visible absorption region (Figure 1) gain their intensity through the mixing of certain b_2 symmetry modes of the 1^2A_2 state with the nearby 2^2B_1 0^0 state (zero vibrational level).[4,5,11,12] The oscillator strength of the $2^2B_1 \leftarrow 1^2B_1$ transition is 1 order of magnitude larger than that of the $1^2A_2 \leftarrow 1^2B_1$ transition (Table 1). This is consistent with the relative electronic transition strength factor of $S^2_{B-X}/S^2_{A-X} = 15$ estimated by Eiden and Weisshaar.[14] The absorption cross section in the visible band can be roughly estimated from the oscillator strength in the UV and visible bands and the absorption cross sections of the UV bands.

$$\sigma(2^2B_1) = \frac{f(2^2B_1)}{f(2^2A_2 \text{ or } 4^2B_1)}\sigma(2^2A_2 \text{ or } 4^2B_1) \qquad (3)$$

where σ is the absorption cross section at the absorption maximum and f is the oscillator strength. The absorption cross sections in the UV band are listed in Table 1. Using eq 3, $\sigma(2^2B_1) = 2.6 \times 10^{-18}$ and 0.9×10^{-18} cm^2 $molecule^{-1}$ are derived on the basis of the 2^2A_2 and 4^2B_1 bands, respectively. The values estimated from the oscillator strengths and UV absorption cross sections are consistent with the value of $\sigma(447.7\ nm) = (2.2 \pm 0.8) \times 10^{-18}$ cm^2 $molecule^{-1}$.

It should be noted that UV−vis absorption spectrum of benzyl radicals has been well studied in the condensed phase. Andrews et al.[17] studied the UV and visible absorption of benzyl radicals in low-temperature (21 K) argon matrices. In the condensed phase, these absorption bands shift to the red side of the gas-phase bands. They measured the absorbance (A) in the UV and visible regions: $A(310.5\ nm) = 0.18$ and $A(449.6\ nm) = 0.010$. In the gas phase, the absorption cross section at 305.3 nm was determined to be ca. 3×10^{-17} cm^2 $molecule^{-1}$ (Table 1).[50,51] Using these values, an absorption cross section of $\sigma(447.7\ nm) = 1.7 \times 10^{-18}$ cm^2 $molecule^{-1}$ is derived. This value supports the value measured in the present work: σ (447.7 nm) $= (2.2 \pm 0.8) \times 10^{-18}$ cm^2 $molecule^{-1}$.

There have been two reported values of $k_3(C_6H_5CH_2 + Cl)$ in the gas phase. Benson and Weissman[49] estimated a rate

constant of 2.1×10^{-10} cm^3 molecule^{-1} s^{-1}. Market and Pagsberg monitored the loss of benzyl radicals in the $C_6H_5CH_3/CCl_4$/Ar photolysis system, and a value of $k_3(C_6H_5CH_2 + Cl) = (6.9 \pm 1.4) \times 10^{-10}$ cm^3 molecule^{-1} s^{-1} was derived.[50] The result from the present work, $k_3(C_6H_5CH_2 + Cl) = (2.5 \pm 1.0) \times 10^{-10}$ cm^3 molecule^{-1} s^{-1}, is in agreement with that reported by Benson and Weissman[49] and is almost identical to those of the reactions of other hydrocarbon radicals with Cl atoms at 298 K (i.e., $k(CH_3 + Cl) = 2.6 \times 10^{-11}$ cm^3 molecule^{-1} s^{-1},[52] $k(C_2H_5 + Cl) = 2.4 \times 10^{-10}$ cm^3 molecule^{-1} s^{-1},[53] $k(C_6H_7 + Cl) = 1 \times 10^{-10}$ cm^3 molecule^{-1} s^{-1},[54] $k(C_6H_5 + Cl) = 1.2 \times 10^{-10}$ cm^3 molecule^{-1} s^{-1} [24]).

Conclusions

We report herein the first absolute measurement of the visible absorption spectrum of the benzyl radical in the region of 445−455 nm using the laser photolysis/cavity ring-down technique. The absorption cross sections reported here will facilitate the quantification of the benzyl radical in future kinetic studies. Benzyl radicals react rapidly with Cl atoms with a rate constant of $k(C_6H_5CH_2 + Cl) = (2.5 \pm 1.0) \times 10^{-10}$ cm^3 molecule^{-1} s^{-1}. This value is in good agreement with the estimated value reported by Benson and Weissman[49] of 2.1×10^{-10} cm^3 molecule^{-1} s^{-1}.

Acknowledgment. This work is supported in part by a Grant-in-Aid from the Ministry of Education, Science, Sports and Culture (no. 13640502 and priority field "Radical Chain Reactions").

References and Notes

(1) Calvert, J. G.; Atkinson, R.; Becker, K. H.; Kamens, R. M.; Seinfeld, J. H.; Wallington, T. J.; Yarwood, G. *Mechanisms of Atmospheric Oxidation of Aromatic Hydrocarbons*; Oxford University Press: New York, 2002.

(2) Porter, G.; Ward, B. *J. Chim. Phys.* **1964**, *61*, 102.

(3) The *x*, *y*, and *z* axes are defined in accordance with Mulliken's recommendation, with the *y* axis in the molecular plane.

(4) (a) Cossart-Magos, C.; Leach, S. *J. Chem. Phys.* **1972**, *56*, 1534. (b) Cossart-Magos, C.; Leach, S. *J. Chem. Phys.* **1976**, *64*, 4006.

(5) Cossart-Magos, C.; Goetz, W. *J. Mol. Spectrosc.* **1986**, *115*, 366.

(6) Heaven, M.; Dimauro, L.; Miller, T. A. *Chem. Phys. Lett.* **1983**, *95*, 347.

(7) Okamura, T.; Charlton, T. R.; Thrush, B. A. *Chem. Phys. Lett.* **1982**, *88*, 369.

(8) Charlton, T. R.; Thrush, B. A. *Chem. Phys. Lett.* **1986**, *125*, 547.

(9) Selco, J. I.; Carrick, P. G. *J. Mol. Spectrosc.* **1989**, *137*, 13.

(10) Fukushima, M.; Obi, K. *J. Chem. Phys.* **1990**, *93*, 8488.

(11) Fukushima, M.; Obi, K. *J. Chem. Phys.* **1992**, *96*, 4224.

(12) Eiden, G. C.; Weinhold, F.; Weisshaar, J. C. *J. Chem. Phys.* **1991**, *95*, 8665.

(13) Eiden, G. C.; Lu, K.-T.; Badenhoop, J.; Weinhold, F.; Weisshaar, J. C. *J. Chem. Phys.* **1996**, *104*, 8886.

(14) Eiden, G. C.; Weisshaar, J. C. *J. Chem. Phys.* **1996**, *104*, 8896.

(15) Yao, J.; Bernstein, E. R. *J. Chem. Phys.* **1997**, *107*, 3352.

(16) Angell, C. L.; Hedaya, E.; McLeod, D. *J. Am. Chem. Soc.* **1967**, *89*, 4214.

(17) Andrews, L.; Miller, J. H.; Keelan, B. W. *Chem. Phys. Lett.* **1980**, *71*, 207.

(18) Miller, J. H.; Andrews, L. *J. Mol. Spectrosc.* **1981**, *90*, 20.

(19) Rice, J. E.; Handy, N. C.; Knowles, P. J. *J. Chem. Soc., Faraday Trans. 2* **1987**, *83*, 1643.

(20) Hiratsuka, H.; Mori, K.; Shizuka, H.; Fukushima, M.; Obi, K. *Chem. Phys. Lett.* **1989**, *157*, 35.

(21) Negri, F.; Orlandi, G.; Zerbetto, F.; Zgierski, M. Z. *J. Chem. Phys.* **1990**, *93*, 600.

(22) Gunion, R. F.; Gilles, M. K.; Polak, M. L.; Lineberger, W. C. *Int. J. Mass Spectrom. Ion Processes* **1992**, *117*, 601.

(23) Park, J.; Lin, M. C. In *Cavity-Ringdown Spectroscopy: An Ultratrace-Absorption Measurement Technique*; Busch, K. W., Busch, M. A., Eds.; ACS Symposium Series 720; American Chemical Society: Washington, DC, 1999; Chapter 13, p 196.

(24) Tonokura, K.; Norikane, Y.; Koshi, M.; Nakano, Y.; Nakamichi, S.; Goto, M.; Hashimoto, S.; Kawasaki, M.; Sulbaek Andersen, M. P.; Hurley, M. D.; Wallington T. J. *J. Phys. Chem. A* **2002**, *106*, 5908.

(25) (a) Becke, A. D. *J. Chem. Phys.* **1993**, *98*, 5648. (b) Becke, A. D. *J. Chem. Phys.* **1992**, 96, 2155. (c) Becke, A. D. *J. Chem. Phys.* **1992**, *97*, 9173.

(26) Lee, C.; Yang, W.; Parr, R. G. *Phys. Rev. B* **1988**, *37*, 785.

(27) (a) Wong, M. W.; Dunning, T. H., Jr. *J. Chem. Phys.* **1993**, 98, 1358. (b) Kendall, R. A.; Dunning, T. H., Jr. *J. Chem. Phys.* **1992**, 96, 6796.

(28) Koch, W.; Holthausen, M. C. *A Chemist's Guide to Density Functional Theory*; Wiley-VCH: Weinheim, Germany, 2000.

(29) Hirata, S.; Head-Gordon, M. *Chem. Phys. Lett.* **1999**, *302*, 375.

(30) Frisch, M. J.; Trucks, G. W.; Schlegel, H. B.; Scuseria, G. E.; Robb, M. A.; Cheeseman, J. R.; Zakrzewski, V. G.; Montgomery, J. A., Jr.; Stratmann, R. E.; Burant, J. C.; Dapprich, S.; Millam, J. M.; Daniels, A. D.; Kudin, K. N.; Strain, M. C.; Farkas, O.; Tomasi, J.; Barone, V.; Cossi, M.; Cammi, R.; Mennucci, B.; Pomelli, C.; Adamo, C.; Clifford, S.; Ochterski, J.; Petersson, G. A.; Ayala, P. Y.; Cui, Q.; Morokuma, K.; Malick, D. K.; Rabuck, A. D.; Raghavachari, K.; Foresman, J. B.; Cioslowski, J.; Ortiz, J. V.; Stefanov, B. B.; Liu, G.; Liashenko, A.; Piskorz, P.; Komaromi, I.; Gomperts, R.; Martin, R. L.; Fox, D. J.; Keith, T.; Al-Laham, M. A.; Peng, C. Y.; Nanayakkara, A.; Gonzalez, C.; Challacombe, M.; Gill, P. M. W.; Johnson, B. G.; Chen, W.; Wong, M. W.; Andres, J. L.; Head-Gordon, M.; Replogle, E. S.; Pople, J. A. *Gaussian 98*, revision A.7; Gaussian, Inc.: Pittsburgh, PA, 1998.

(31) Kong, J.; White, C. A.; Krylov, A. I.; Sherrill, C. D.; Adamson, R. D.; Furlani, T. R.; Lee, M. S.; Lee, A. M.; Gwaltney, S. R.; Adams, T. R.; Ochsenfeld, C.; Gilbert, A. T. B.; Kedziora, G. S.; Rassolov, V. A.; Maurice, D. R.; Nair, N.; Shao, Y.; Besley, N. A.; Maslen, P. E.; Dombroski, J. P.; Dachsel, H.; Zhang, W. M.; Korambath, P. P.; Baker, J.; Byrd, E. F. C.; Van Voorhis, T.; Oumi, M.; Hirata, S.; Hsu, C. P.; Ishikawa, N.; Florian, J.; Warshel, A.; Johnson, B. G.; Gill, P. M. W.; Head-Gordon, M.; Pople, J. A. *J. Comput. Chem.* **2000**, *21*, 1532.

(32) Lange, S.; Luther, K.; Rech, T.; Schmoltner, M.; Troe, J. *J. Phys. Chem.* **1994**, *98*, 6509.

(33) Kajii, Y.; Obi, K.; Tanaka, I.; Nakashima, N.; Yoshihara, K. *J. Chem. Phys.* **1987**, *86*, 6115.

(34) Damm, M.; Decker, F.; Hippler, H.; Rink, G. *Phys. Chem. Chem. Phys.* **1999**, *1*, 81.

(35) Park, J.; Bersohn, R.; Oref, I. *J. Chem. Phys.* **1990**, *93*, 5700.

(36) Hippler, H.; Lindemann, L.; Troe, J. *Ber. Bunsen-Ges. Phys. Chem.* **1988**, *92*, 440.

(37) Brand, U.; Hippler, H.; Lindemann, L.; Troe, J. *J. Phys. Chem.* **1990**, *94*, 6305.

(38) Calculated from ref 34 in eq 3.

(39) Ichimura, T.; Mori, Y. *J. Chem. Phys.* **1972**, *57*, 1677.

(40) Muller-Markgraf, W.; Troe, J. *J. Phys. Chem.* **1988**, *92*, 4899.

(41) O'Keefe, A.; Deacon, D. A. G. *Rev. Sci. Instrum.* **1988**, *59*, 2544.

(42) Boyd, A. A.; Noziere, B.; Lesclaux, R. *J. Phys. Chem.* **1995**, *99*, 10815.

(43) Heckmann, E.; Hippler, H.; Troe, J. *Symp.* (*Int.*) *Combust.* [*Proc.*] **1996**, *26*, 543.

(44) Baulch, D. L.; Cobos, C. J.; Cox, R. A.; Frank, P.; Hayman, G.; Just, Th.; Kerr, J. A.; Murrells, T.; Pilling, M. J.; Troe, J.; Walker, R. W.; Warnatz, J. *J. Phys. Chem. Ref. Data* **1994**, *23*, 847.

(45) Zhang, H. X.; Ahonkhai, S. I.; Back, M. H.*Can. J. Chem.* **1989**, *67*, 1541.

(46) Holt, P. M.; Kerr, J. A. *Int. J. Chem. Kinet.* **1977**, *9*, 185.

(47) Baulch, D. L.; Duxbury, J.; Grant, S. J.; Montague, D. C. *J. Phys. Chem. Ref. Data* **1981**, *10* (Supplement).

(48) Noziere, B.; Lesclaux, R.; Hurley, M. D.; Dearth, M. A.; Wallington, T. J. *J. Phys. Chem.* **1994**, *98*, 2864.

(49) Benson, S. W.; Weissman, M. *Int. J. Chem. Kinet.* **1982**, *14*, 1287.

(50) Market, F.; Pagsberg, P. *Chem. Phys. Lett.* **1993**, *209*, 445.

(51) Ikeda, N.; Nakashima, N.; Yoshihara, K. *J. Phys. Chem.* **1984**, *88*, 5803.

(52) Timonen, R.; Kalliorinne, K.; Koskikallio, J. *Acta Chem. Scand. Ser. A* **1986**, *40*, 459.

(53) Kaiser, E. W.; Rimai, L.; Wallington, T. J. *J. Phys. Chem.* **1989**, *93*, 4094.

(54) Berho, F.; Rayez, M.-T.; Lesclaux, R. *J. Phys. Chem. A* **1999**, *103*, 5001.